Calculation of Inlet Flows Applied to Ducted Propellers

R. J. Weetman* and D. E. Cromack†
University of Massachusetts, Amherst, Mass.

This investigation concerns inlet flow calculations applied to ducted propellers. The analysis is classified as that of an inlet flow since the ducted propeller wake is assumed to be at a constant diameter. A closed distribution of ring vortices is used to describe the duct and wake. By forming a closed distribution, the velocity can be equated directly to the vorticity. With this representation, a singular integral equation of the first kind is formulated for the vorticity in terms of the streamline enclosing the duct and wake. Several techniques incorporated in the numerical solution of this integral equation are presented. This analysis provides a needed solution for ducted propellers operating at low speeds and statically, as well as at high speeds. Experimental results for the velocity distribution are shown to agree well with this analysis. In addition, excellent agreement is obtained using this method for the classical flow around a sphere.

Nomenclature

$A_{i,j}$ = influence function
c = leading-edge expansion coefficient
C_p = pressure coefficient
$E(k)$ = complete elliptic integral of the 2nd kind
f = defined by Eq. (6)
F_i = defined by Eq. (11)
II = collocation point index
k = modulus of elliptic integral
$K(k)$ = complete elliptic integral of the 1st kind
KK = integration point index
L = nondimensionalizing variable
N = number of collocation points
r,r' = radial coordinate
r_j = radial coordinate at collocation point
R_{ite} = radius of inside trailing edge
R_∞ = radius of wake at $x = \infty$
s,s' = curvilinear coordinate
s_i = curvilinear coordinate at collocation point
v = velocity
$\bar{v}_e$ = average velocity at duct exit plane
v_∞ = velocity inside wake at $x = \infty$
V = freestream velocity
x,x' = axial coordinate
α = slope angle at singularity
γ = vorticity
γ_j = vorticity in j interval
ΔP_0 = pressure drop across propeller
κ = kernel defined by Eq. (2)
$\bar{\sigma}$ = half chord length of singular subinterval
ϕ,ϕ' = transformed coordinate defined by Eq. (15)
ϕ_{te} = ϕ coordinate at trailing edge
Ψ = stream function
Ψ_0 = stream function of duct

Introduction

AN inlet flow calculation applied to ducted propellers is considered in this investigation. Previous work on ducted propellers has been reviewed extensively by Weetman and Cromack,[1] Weissinger and Maass,[2] Morgan and Caster[3] and Sacks and Burnell.[4] Most of the past work has incorporated a linear analysis which is adequate only for high speed conditions when the induced velocities are much smaller than the free stream velocity. References 5 and 6 provide working examples for the high speed case.

To date, there has not been a satisfactory analysis for low speed conditions where ducted propellers are used most (i.e., deep sea submersibles, tugboats and VTOL aircraft). Three papers that have made approximations for the low speed and static cases are by Greenberg and Ordway,[7] Kriebel[8] and Chaplin.[9] Since the first two analyses both utilize a distribution of vortices on a constant diameter cylinder, they minimize the dependence on the duct shape. Chaplin does present a nonlinear analysis that could be used for a duct with thickness. Most of his work, however, deals with ducts of zero thickness, therefore, his numerical scheme has limitations that prohibit accurately describing a so-called thick duct. The program requires a leading edge singularity and does not allow closing of the airfoil profile.

This paper describes an analysis for the ducted propeller that is applicable for low speed and static conditions as well as for high speeds. The analysis incorporates the notion that when a continuous vortex distribution is used to represent a closed body, then one can equate directly the vorticity to the velocity on the body. This concept was developed by Martensen[10] for two-dimensional flow through a cascade. The vortex distribution along with the freestream velocity are used to describe the streamline enclosing the body, thus forming a singular integral equation of the first kind.

In order to apply this closed body formulation for the case of ducted propellers, a double branched wake that meets at infinity is postulated. This wake model, representing a velocity discontinuity, is in accord with the use of a constant pressure actuator disk model for the propeller. The branches of the wake are placed at constant diameters originating at the trailing edge. Hence the wake is modeled as a cylindrical duct and the analysis can thus be classified as that of an inlet flow. This constant diameter approximation does not greatly influence the velocity distribution on the duct for the following reasons. First, slipstream contraction is small for ducts with chord to diameter ratios greater than 0.4 and secondly, vortices have predominantly a local influence.

Several techniques are developed to aid in the numerical solution of this problem. These methods include formulation of a diagonal matrix, expansion of the leading edge region, integration schemes, and the interpolation between the points describing the duct shape.

The analysis is then compared to the classical solution for flow around a sphere and to experimental results obtained by the authors and by others.

Theory

First, a potential flow solution for axisymmetric bodies is formulated which is then applied to the problem of ducted propellers.

Potential Flow

A potential flow can be described by a distribution of vorticity along with a freestream velocity. The following

Received January 8, 1973; revision received June 4, 1973. This research was sponsored by the Office of Naval Research under ONR Contract N00014-68-A-0146 with the University of Massachusetts School of Engineering.

Index categories: Propulsion System Hydrodynamics; Marine Propulsion.

*Research Assistant, Department of Mechanical and Aerospace Engineering; presently, Senior Engineer, Process Research Center, Corning Glass Works, Corning, N.Y. Member AIAA.

† Associate Professor, Department of Mechanical and Aerospace Engineering. Member AIAA.

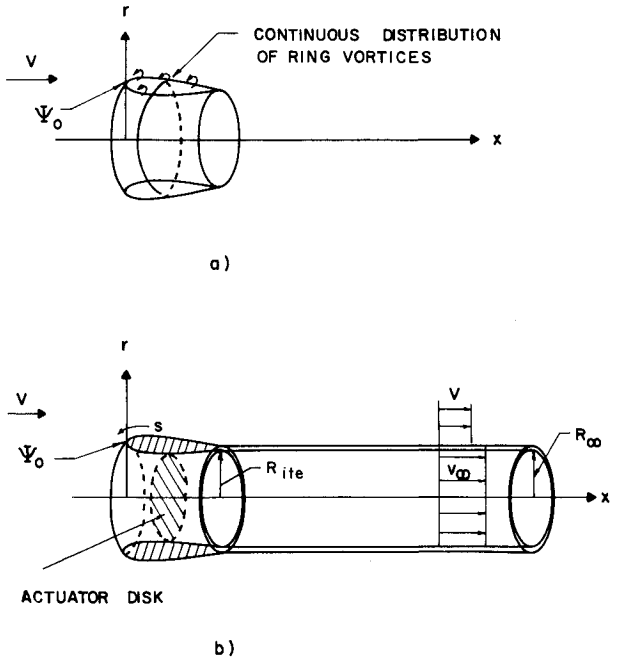

Fig. 1 Axisymmetric body and ducted propeller.

stream function contribution from a continuous vortex distribution is derived by integrating the velocity obtained from the Biot-Savart law as formulated by Küchemenn and Weber[11]

$$\Psi = \int_s \kappa(s,s')\gamma(s')ds' \tag{1}$$

where

$$\kappa(s,s') = (1/2\pi)\{[x(s) - x(s')]^2 + [r(s) + r(s')]^2\}^{1/2} [(1 - k^2/2)K(k) - E(k)] \tag{2}$$

$$k^2 = \frac{4\, r(s)r(s')}{[x(s) - x(s')]^2 + [r(s) + r(s')]^2} \tag{3}$$

$K(k)$ is the complete elliptic integral of the 1st kind. $E(k)$ is the complete elliptic integral of the 2nd kind.

Adding the contribution of the freestream velocity to the above, the total stream function becomes

$$\Psi = \int_s \kappa(s,s')\gamma(s')ds' + \int_0^{r(s)} V(r')r'dr' \tag{4}$$

Rewriting Eq. (4) and defining ψ_0 as the streamline enclosing the body (Fig. 1a) the following is obtained:

$$\int_s \kappa(s,s')\gamma(s')ds' = \Psi_0 - \int_0^{r(s)} V(r')r'dr' \tag{5}$$

Defining $f(s)$ as

$$f(s) \equiv \Psi_0 - \int_0^{r(s)} V(r')r'dr' \tag{6}$$

which, for constant V, becomes

$$f(s) = \Psi_0 - V[r(s)]^2/2 \tag{7}$$

Thus, Eq. (5) reduces to

$$\int_s \kappa(s,s')\gamma(s')ds' = f(s) \tag{8}$$

which is a singular integral equation of the 1st kind for the vorticity distribution, $\gamma(s)$.

The general approach used in airfoil theory would be to solve Eq. (8) for the vorticity distribution which would then be used to determine the velocity by means of the Biot-Savart law. A simpler analysis, if the vortex distribution is closed, is to equate the velocity to the vorticity directly. This identity, with proper regard for the sign of the vorticity, was used by Martensen[10] in the solution of two-dimensional flow around cascades. He showed that the velocity within a closed vorticity distribution is identically zero. This condition, along with the fact that a velocity jump across any vortex sheet is equal to the vorticity, enables the velocity to be equated to the vorticity.

This identity between the velocity and vorticity is employed in the solution of Eq. (8). The solution of Eq. (8) is accomplished by a collocation scheme that approximates the function $\gamma(s)$ with constant values γ_j in intervals over the boundary s, i.e.,

$$\sum_{j=1}^{N} A_{i,j}\gamma_j = F_i \qquad (i = 1,2, \ldots, N) \tag{9}$$

where

$$A_{i,j} \equiv \int_{\text{interval}_j} \kappa(s_i,s')ds' \tag{10}$$

$$F_i \equiv f(s_i) \tag{11}$$

The quantities $A_{i,j}$ and γ_j, called influence coefficients

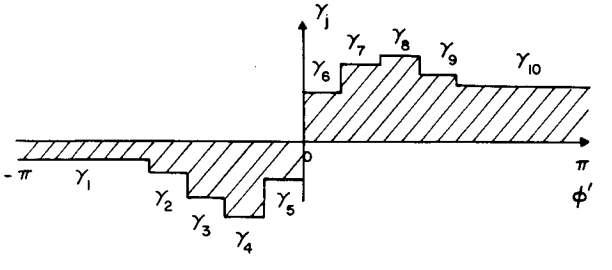

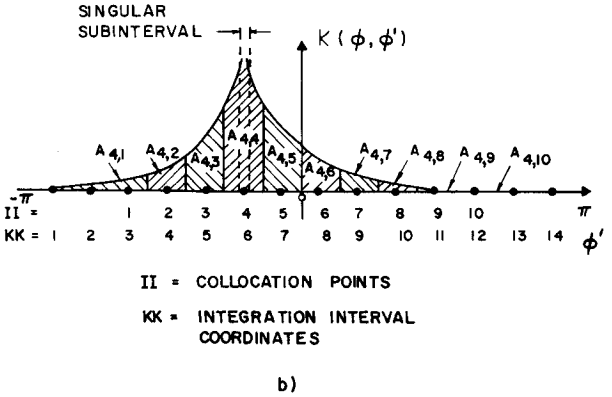

Fig. 2 Vorticity and influence functions.

and the vorticity in interval j, respectively, are illustrated in Fig. 2. Since the kernel $\kappa(s_i,s')$ is singular when $s_i = s'$, a suitable expansion and and integration over a singular subinterval is performed. Integration over an interval of chord length equal to $2\bar{\sigma}r_j$ gives

$$A_{j,j_{\text{sing.}}} = \frac{r_j^2}{\pi}\left[\ln\frac{\bar{\sigma}}{8}\left\{-\bar{\sigma} + \left(\frac{\sin^2\alpha}{24} - \frac{1}{16}\bar{\sigma}^3\right\} - \bar{\sigma} + \left(\frac{5}{72}\sin^2\alpha\right)\bar{\sigma}^3\right]\right. \quad (12)$$

This result is added to the nonsingular part of the $A_{j,j}$ influence coefficient, which is calculated numerically by gaussian integration.

Detailed calculations of Eq. (12) are given by Weetman and Cromack.[12]

Ducted Propellers

Application of the analysis previously developed is shown in Fig. 1b for a ducted propeller. The ducted propeller exhibits a trailing wake caused by the presence of the propeller. A constant pressure actuator disk representation for the propeller, results in the wake appearing as a velocity discontinuity originating at the duct trailing edge and extending to infinity. The continuous closed vorticity distribution required in the above analysis is formed by the duct and a double branched wake joined at infinity. Since the duct trailing edge normally has a finite thickness, the two branches of the wake are extended from these outside and inside trailing edges, respectively. If the theoretical duct shape does not have a finite trailing edge thickness, then a suitable thickness (approximately 1% of the inside trailing edge radius) must be included in the solution. A separation between the branches is utilized for this analysis since it represents what happens physically in a real fluid, i.e., a finite thickness to the wake, and it produces a more diagonal matrix, which aids in the numerical solution of the problem.

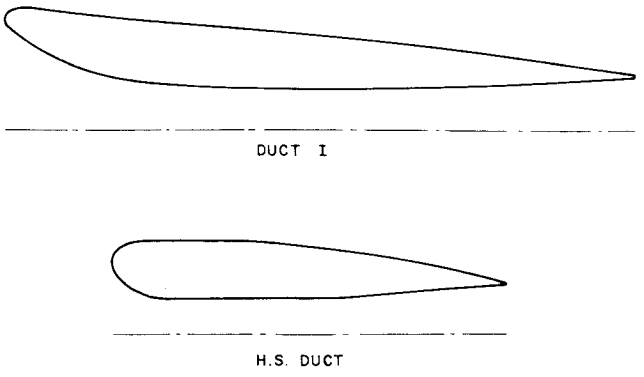

Fig. 4 Duct profiles.

The two branches of the wake are placed at constant diameters extending to infinity. A constant diameter approximation is valid since the final radius of the slipstream, R_∞, does not vary much from the inside trailing edge radius. This is indicated by Chaplin's[9] results for conical and parabolic cambered ducts of zero thickness. If ducts with total diffuser angles less than 7° are considered, then the final radius, R_∞, is less than 1¼% greater than the trailing edge radius. An angle of seven degrees was chosen as an upper limit for the diffuser angle for ducts that would be practical in a real flow. This is the angle around which optimum diffuser recovery is achieved for diffusers in wind tunnels.[13]

In the present formulation for the ducted propeller, the duct trailing edge condition (analogous to the Kutta condition) is satisfied by having a smooth continuous transition from the duct to the wake.

In the solution of Eq. (9), the last collocation point used on the wake branches occurs at $x \cong 4$, where all the dimensions have been normalized with respect to the inside

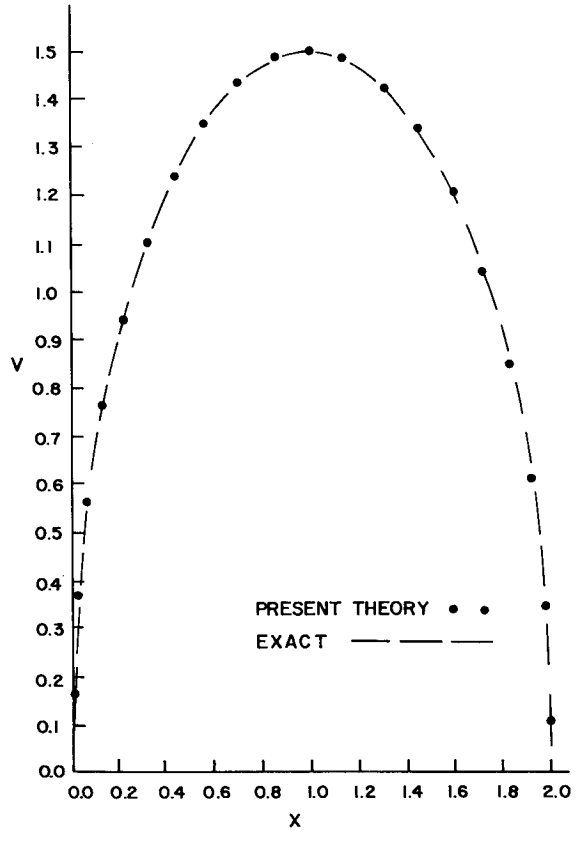

Fig. 3 Velocity around sphere.

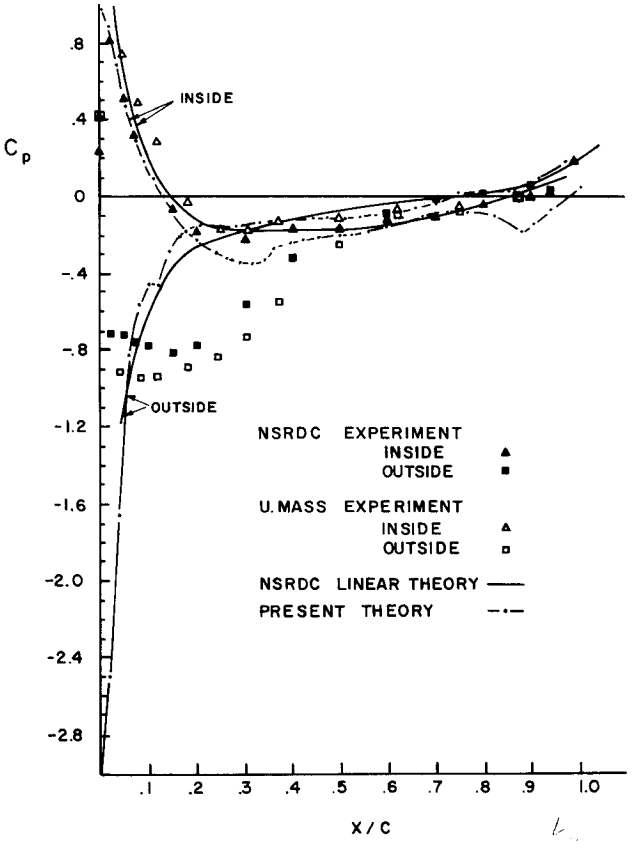

Fig. 5 Pressure distribution on duct I without propeller.

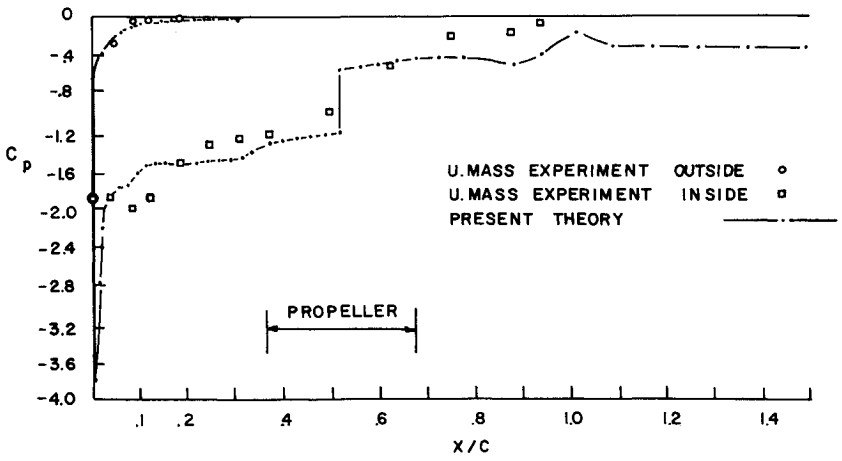

Fig. 6 Pressure distribution on duct I for static condition.

trailing edge radius. At this value, the flow has been found to be sufficiently close to its asymptotic solution, i.e., $x = \infty$. This was also shown by Chaplin.[9]

The required inputs for the solution of Eq. (9), in addition to the duct coordinates, are the freestream velocity (V) and the value of the streamline (ψ_0) that represent the duct and wake boundaries.

By the definition of the stream function,

$$\Psi = \int_0^r vr'dr' \tag{13}$$

the boundary streamline can be related to the final wake velocity (v_∞) and radius (R_∞) as follows:

$$\Psi_0 = v_\infty R_\infty{}^2/2 \tag{14}$$

Numerical Techniques

Following is a discussion of some of the numerical techniques used to obtain solutions to Eq. (9).

Matrix

In the solution of the system of equations represented by Eq. (9), it is desirable to obtain a diagonal matrix of coefficients, $A_{i,j}$. A diagonal matrix, defined here as one which has its diagonal elements larger than any of its off diagonal terms, has considerably less roundoff error than a nondiagonal matrix in the solution of a system of equations. This is especially true, as in the present case, when most of the coefficients of the matrix are nonzero and a matrix inversion scheme is used.

As illustrated in Fig. 2, the interval for each constant value of γ_j (except the two end points which have the kernel $[\kappa(\phi,\psi)]$ approaching zero) is centrally located over the collocation point. Thus, with the integration interval for the $A_{j,j}$ influence coefficient equally spaced around the singularity, the coefficient $A_{j,j}$ will have the largest value. This result produces the desired diagonal matrix.

Leading Edge Expansion

It is desirable to obtain a transformation from the s-coordinate that would expand the leading edge region because of the high velocity gradients present in that region. By the expansion of the leading edge region, the favorable result of compressing the wake branches that extend to infinity would also be achieved. The following transformation was formulated to obtain this leading edge expansion:

$$\phi = 2 \tan^{-1}(cs/L) \tag{15}$$

where c is a nondimensional expansion coefficient and L, set equal to the inside trailing edge radius, is used to nondimensionalize s. Eqs. (7) and (10) thus become

$$f(\frac{s}{L}) = \frac{\Psi_0}{L^3} - \frac{1}{2}(\frac{V}{L})[\frac{r(s/L)^2}{L}] \tag{16}$$

$$A_{i,j} = \int_{\substack{j \\ \text{interval}}} \kappa(\frac{s_i}{L}, \frac{s'}{L}) d(\frac{s'}{L}) \tag{17}$$

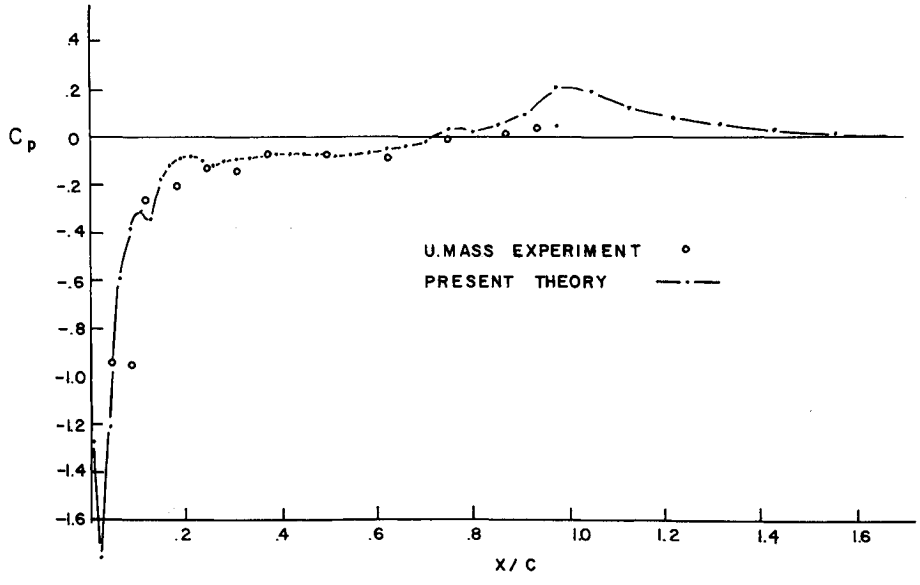

Fig. 7 Pressure distribution on outside of duct I at low speed.

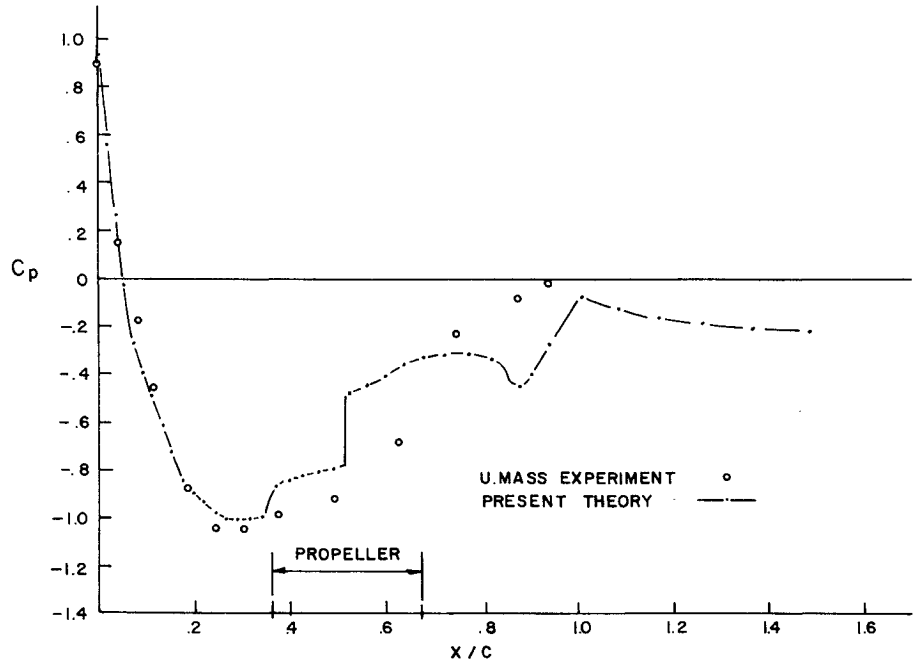

Fig. 8 Pressure distribution on inside of duct I at low speed.

By the use of Eq. (15), the limits of the wake at $s = \pm\infty$ become $\phi = \pm\pi$ while the coefficient, c, is used to expand the leading edge.

The value of ϕ at the trailing edge determines the magnitude of the expansion coefficient, c. For a value of ϕ_{te} = 2.0, a good distribution of collocation points is obtained over the duct, including the leading edge and wake. If more detail is desired around the leading edge, ϕ_{te} is increased to approximately 2.9, with a corresponding decrease in the accuracy of the wake. This decrease in accuracy does not alternately affect the increased accuracy in the expanded region (i.e., leading edge) because of the local effect of a vorticity distribution.

From the preceding, a method of increasing the accuracy of a solution would be to calculate the vorticity with ϕ_{te} equal to 2.9 for detail near the leading edge and with ϕ_{te} equal to 1.0 for detail in the wake. Obviously, other ways to increase the accuracy of the solution would be to increase the number of collocation points or increase the number of integration intervals.

Using the transformation, ϕ, the expression for the influence coefficients become

$$A_{i,j} = \int_{\substack{j \\ \text{interval}}} \frac{\kappa(\phi,\phi')}{[2c\cos^2(\phi'/2)]} d\phi' \qquad (18)$$

Integration

Except for the singular subinterval, the integration involved in calculating $A_{i,j}$ [Eq. (18)] is done numerically by three-point gaussian integration. The computer program implementing this analysis allows the numerical accuracy of the integration to be increased by increasing the number of gaussian intervals. This increase is accomplished without requiring an increase in the number of collocating points or duct coordinates.

In an attempt to reduce computer time, simpson integration was considered because it requires fewer coordi-

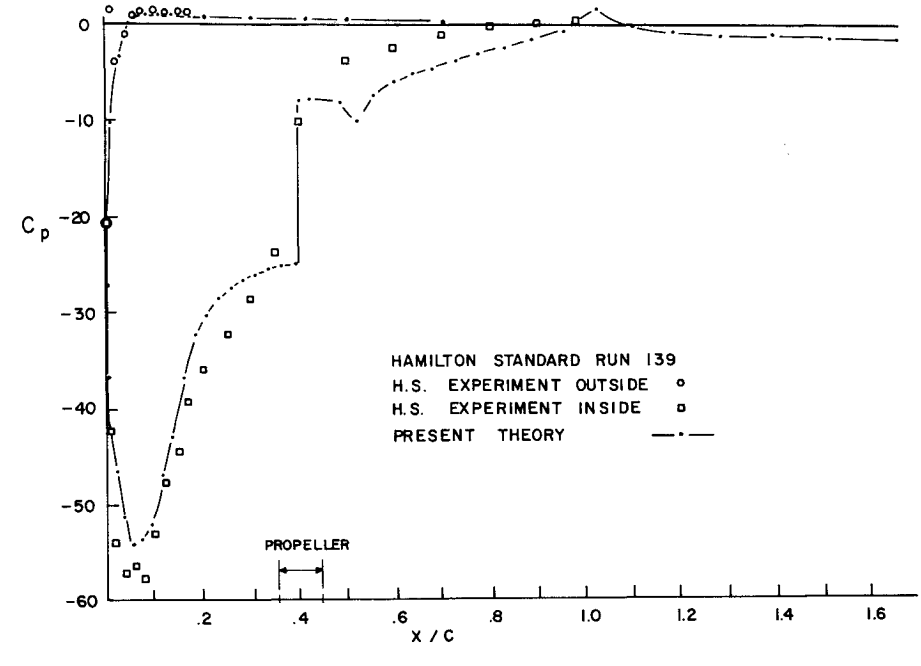

Fig. 9 Pressure distribution on H.S. duct at low speed.

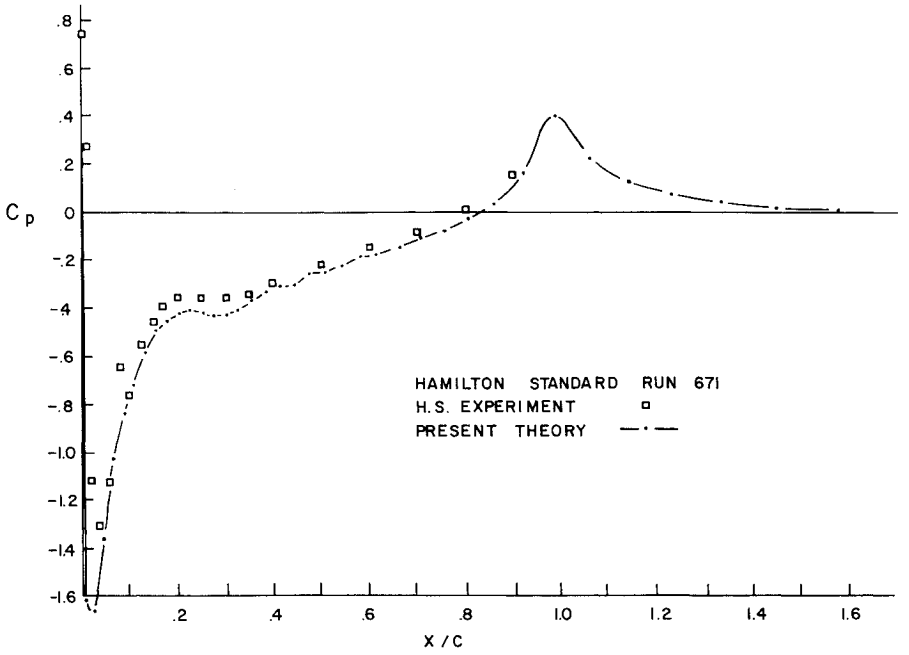

Fig. 10 Pressure distribution on outside of H.S. duct at high speed.

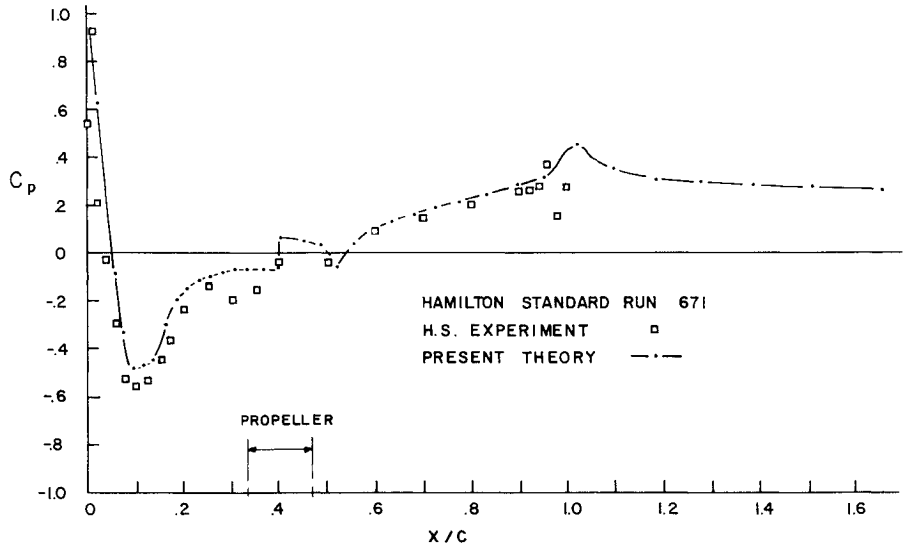

Fig. 11 Pressure distribution on inside of H.S. duct at high speed.

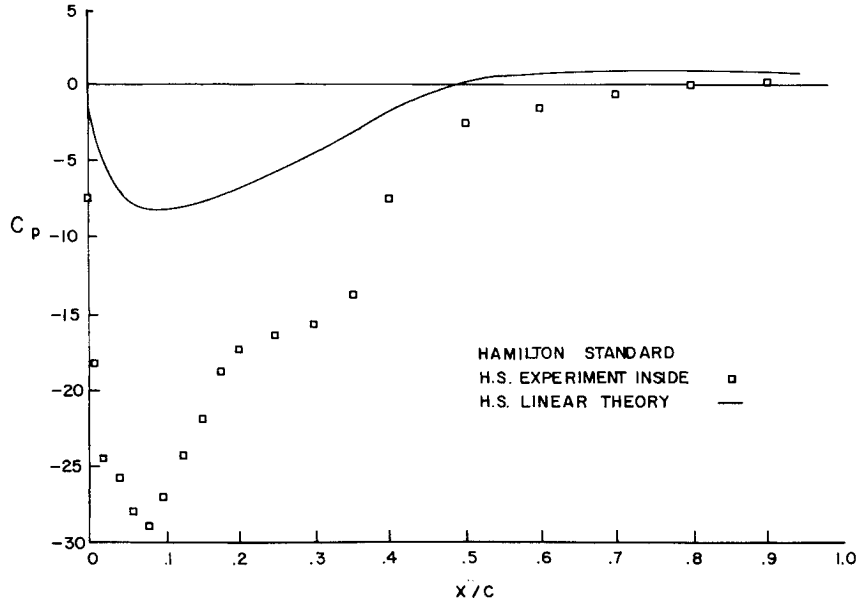

Fig. 12 Comparison of H.S. linear theory with experiment at low speed.

nates than gaussian integration. This is especially important in the present analysis since three coordinate transformations are employed. Unfortunately, when the number of simpson integration intervals was increased to give the same accuracy obtained from gaussian integration, the Simpson method required twice as much computer time.

Duct Shape Interpolation

An interpolation scheme for the duct profile was used for the following reasons. First, it simplifies inputting the duct coordinates by not restricting how the points are distributed, and second, it does not require any specified number of points. The only guideline for inputting the coordinates is to use more points in regions where the curvature has the greatest rate of change. When using the interpolation scheme the integration intervals and expansion coefficient can be changed without inputting new duct coordinates.

Three interpolation schemes were investigated. First, a high order polynomial, of the order of ten, was tried and found to be totally unreliable because of the roundoff error. The normal roundoff error from a high order polynomial was probably exaggerated by the closeness of the ordinates describing the duct. The second method attempted, which had negligible roundoff error, was the use of only a second order polynomial, i.e., parabola, between every three points on the duct. This method also proved to be unreliable for arbitrarily spaced points. Near the leading edge where the first two of the three interpolating points were grouped close together, the disadvantage of this scheme was apparent. The resulting second order polynomial produced a predominant maximum between the second and third points which was clearly not representative of the duct shape. Interpolating with a circle between every three points provided a successful scheme that overcame the difficulties described. This was possible for a duct, even though it is a double-valued function. Since an infinite slope occurs only at the leading edge, this is used as a starting point for the interpolating functions. A straight line is used for interpolating if the three points form a straight line or if the difference in the slope of the line between the first two points and the last two points is less than a specified value (presently equal to 0.01). Details of this circle interpolation are given by Weetman and Cromack.[12]

Comparison with an Exact Solution

The present analysis, i.e., step collocation method, was used to calculate the flow around a sphere. Since the computer program requires a hole in a body of revolution, a unit sphere with a 0.001 diam hole was specified in the program for the limiting case of $\psi_0/V = 0.5$ (i.e., no propeller). Results of this calculation are shown in Fig. 3 and exhibit no noticeable difference when compared with the exact solution.

Comparison with Experiments

This analysis is compared with experimental results from two ducted propeller configurations. Duct I, as shown in Fig. 4, was used by the authors at the University of Massachusetts[12] (UMASS) and by the Naval Ship Research and Development Center[14] (NSRDC). One of the ducts used by Hamilton Standard (H.S.) in their testing program,[15] shown in Fig. 4, is also to be used for comparison.

The analysis discussed in the previous sections calculates the velocity distribution, from which the pressure coefficient is obtained, on a duct and wake. This calculation is done for a given duct shape, freestream velocity and boundary streamline, i.e. volume flow through the duct. Thus, in order to compare experimental results with the analysis, the value of the boundary streamline, ψ_0, for the experimental conditions has to be obtained. This is determined by the following relationship:

$$\Psi_0 = R_{ite}{}^2 \bar{v}_e/2 \tag{19}$$

where $\bar{v}_e$ is the average exit velocity between the centerbody and the radius at the inside trailing edge of the duct, R_{ite}. A velocity traverse across the duct exit plane is required to calculate this average velocity. By using the average exit velocity over the entire exit plane, i.e. by means of Eq. (19), the influence of a small centerbody, i.e. radius less than 25% of the duct radius, is considered. Also, although the analysis assumes an actuator disk representation for the propeller loading, the averaging of the exit velocity to obtain ψ_0 should aid in smoothing out the small variations in propeller loading for comparison purposes.

Figures 5–12 present pressure distributions for the above ducts under various conditions. The pressure coefficients plotted are normalized with respect to the freestream velocity head except for results of the static case which is based on the velocity head from the average exit velocity.

Since the present analysis calculates the velocity in the wake, as well as the velocity on the duct, this is also indicated in Figs. 6–12. Although the asymptotic value of the velocity in the wake approaches the correct value determined by the stream function, the pressure coefficient on the inside surface does not always approach zero. This disagreement in the wake could be caused by first, neglecting the slipstream contraction or secondly, the use of an actuator disk representation for the propeller. Another possible source of error that strongly affects this asymptotic pressure coefficient is the determination of the average exit velocity. A change of 5% in this velocity for duct I operating at low speed produced a 50% shift in the final pressure coefficient because the coefficient was approaching zero.

Results using duct I without a propeller are presented in Fig. 5. For comparison, experimental and linear theoretical results from NSRDC[14] are also shown. Their experimental results, taken with the same shaped duct, agree fairly well, although separation occurs on the outside of the duct, with the present tests.[12] The general trends predicted by the present method agree with those of the linear theory for this case. The present analysis, however, predicts expected detail in the pressure distribution. As an example, on the outside surface at $x/c \cong 0.2$ the pressure overshoots, which is caused by a concave section in the duct as seen in Fig. 4. A drop in the pressure also occurs on the inside of the duct at $x/c \cong 0.3$ caused by the transition from a curved to a straight section on the duct. This transition drop is also seen near the duct trailing edge.

Duct I results for the static condition are shown on Fig. 6. The high velocity predicted by the analysis of the leading edge was not realized because of the slight flow separation as shown by the experimental data. Except for this region, the results of the pressure on the duct agree fairly well. The pressure jump, representing the propeller in Fig. 6, was obtained from the experimental pressure rise in the region shown for the propeller.

Experiments were also run for the low speed case and are shown in Figs. 7 and 8. Slight separation at the leading edge for this case also causes a discrepancy between the calculated high velocity and experimental results in this region. Furthermore, the flow does not follow the concave section of the duct at $x/c \cong 0.2$. These two areas, where differences occur between the analysis and experimental results, actually show the value of the present theory. The

advantage of this analysis is that it can be used to select duct shapes from their calculated pressure distributions. Thus, the high adverse pressure gradients predicted for this low speed case would indicate that duct I might separate, as indeed it does, in these two regions. Therefore, a duct profile with a larger leading edge radius than duct I, and one without concave sections, would probably be a better choice for low speed operation. Results on the inside surface of duct I are shown in Fig. 8. For this run, the prediction of the pressure near the inside trailing edge varies considerably from the experimental data. Additional reasons for this discrepancy, other than the slipstream contraction and actuator disk assumptions discussed earlier, might be the large axial distance occupied by the propeller and the possibility of separation near the trailing edge.

Experimental results from Hamilton Standard,[15] H.S., are presented in Figs. 9-12. Good agreement is obtained for a low speed case, Fig. 9, and for a high speed case, Figs. 10 and 11 when compared to the present analysis. Because the flow does not separate near the leading edge on the H. S. duct, better agreement is obtained than from duct I. The small pressure drop predicted aft of the propeller in Figs. 9 and 11 is caused by the transition from the straight to the curve section on the duct. Unfortunately, the experimental results do not indicate this, probably because of the close proximity of the propeller. A pressure drop caused by a similar transition on the outside of the duct, at $x/c \cong 0.25$ on Fig. 10, is indicated by the experimental as well as by the theoretical results. In order to show the value of this analysis, a comparison between Hamilton Standard's[16] linear analysis and the experimental data for their duct is shown in Fig. 12. This illustrates clearly that a linear analysis can not be used for the low speed case. In comparison, the present analysis gives very good results for the same duct, as shown in Fig. 9, for this low-speed condition.

Conclusion

A potential flow solution to the equations governing inlet flow has been developed and applied to ducted propellers. This analysis can be employed for any arbitrary shaped duct and used for ducted propellers operating at low speeds and statically, as well as at high speeds. By comparing the analysis with experimental results for these three operating conditions, agreement has been achieved to substantiate this solution.

The analysis can also be used to calculate the flow about general bodies of revolution. Verification of this was shown by the excellent agreement of the analysis as compared to the classical flow around a sphere.

For this analysis, the concept of using a closed vortex distribution to represent a body was demonstrated for inlet flows and ducted propellers. This was made possible by forming the closed vortex distribution from the duct and a postulated double branched wake, initiated at the duct trailing edge and closed at infinity.

The following techniques, with their resulting effects, were developed to aid in the numerical solution of this problem. 1) By a suitable arrangement of a collocation method, a diagonal matrix was formed which produced good matrix inversion accuracy. 2) By determining a suitable leading-edge expansion transformation, the accuracy of the solution in the leading-edge region can be increased to any desired extent. 3) By the use of a series of circle functions to interpolate between the specified duct coordinates, there results: no restrictions on the arrangement of the specified duct coordinates; no changes in the duct coordinates required if the numerical integration accuracy is varied; and no changes in the duct coordinates needed if the leading edge region is expanded.

The resulting computer program[12] implementing the present analysis contains the following advantageous features: 1) reasonable computer time, i.e., 3 to 10 min on a CDC 3800; 2) ease of inputting arbitrary duct coordinates; 3) convenience of changing the number of collocation points, the desired accuracy of integration, and the leading-edge expansion coefficient; 4) up to 10 flow conditions can be calculated simultaneously; 5) expression of the freestream velocity either as a constant or as a function of the radial coordinate; 6) inclusion of a finite thickness to the duct trailing edge.

Since ducted propellers are used mainly for low speed operations of deep sea submersibles, tugboats and VTOL aircraft, this investigation has produced a needed analysis for these applications.

References

[1]Weetman, R. J. and Cromack, D. E., "Ducted Propellers—A Review and Description of Current Investigation," Rept. THEMIS-UM-70-1, Contract ONR-N00014-68-A-0146-12, 1970, Univ. of Massachusetts, Amherst, Mass.

[2]Weissinger, J. and Maass, D., "Theory of the Ducted Propeller. A Review," 7th Symposium on Naval Hydrodynamics, Rome, Aug. 25-30, 1968.

[3]Morgan, W. B. and Caster, E. B., "Comparison of Theory and Experiment on Ducted Propellers," 7th Symposium on Naval Hydrodynamics, Rome, Aug. 25-30, 1968.

[4]Sacks, A. H. and Burnell, J. A., "Ducted Propellers—A Critical Review of the State of the Art," *Progress in Aeronautical Sciences*, Vol. 2, Pergamon Press, New York, 1962.

[5]Caster, E. B., "A Computer Program for Use in Designing Ducted Propellers," Rept. 2507, Naval Ship Research and Development Center, Nov. 1967, Washington, D.C.

[6]Kaskel, A. L., Ordway, D. E., Hough, G. R., and Ritter, A., "A Detailed Numerical Evaluation of Shroud Performance for Finite Bladed Ducted Propellers," TAR-TR-639, Dec. 1963, Therm Advanced Research, Ithaca, N.Y.

[7]Greenberg, M. D. and Ordway, D. E., "The Ducted Propeller in Static and Low-Speed Flight," TAR-TR-6407, Oct. 1964, Therm Inc., Ithaca, N.Y.

[8]Kriebel, A. R., "Theoretical Investigation of Static Coefficients, Stability Derivatives and Interference for Ducted Propellers," Vidya Rep. 112 1964, Vidya Research and Development, Palo Alto, Calif.

[9]Chaplin, H. R., "A Method for Numerical Calculation of Slipstream Contraction of a Shrouded Impulse Disc in the Static Case with Application to Other Axisymmetric Potential Flow Problems," Rept. 1857, June 1964, David Taylor Model Basin, Washington, D.C.

[10]Martenson, E., "Calculation of the Pressure Distribution on a Cascade of Thick Airfoils by Means of Fredholm Integral Equations of the Second Kind," communications from the Max Planck Institute for Fluid Mechanics and the Aerodynamic Experimental Station, No. 23, 1959, translation by R. J. Weetman given in NASA TT F-702.

[11]Küchemann, D. and Weber, J., *Aerodynamics of Propulsion*, 1st ed., McGraw-Hill, New York, 1953, pp. 305-310.

[12]Weetman, R. J. and Cromack, D. E., "Calculation of Inlet Flows by Means of a Closed Vorticity Distribution Applied to Ducted Propellers," Rept. UM-72-11, Contract ONR-N00014-68-A-0146-6, -12 (AD 754-114), 1972, Univ. of Amherst, Mass.

[13]Pope, A. and Harper, J. J., *Low-Speed Wind Tunnel Testing*, Wiley, New York, 1966, p. 41.

[14]Morgan, W. B. and Caster, E. B., "Prediction of the Aerodynamic Characteristic of Annular Airfoils," Rept. 1830, Jan. 1965, David Taylor Model Basin, Washington, D.C.

[15]Black, D. M. and Wainauski, H. S., "Hamilton Standard Shrouded Propeller Test Program," Rept. HSER 4348, Vol. 1 & 2, May 1967, Hamilton Standard, Windsor Locks, Conn.

[16]Worobel, R. and Peracchio, A. A., "Hamilton Standard Shrouded Propeller Test Program, Method Development," Rept. HSER 4776, Vol. 1, Jan. 1968, Hamilton Standard, Windsor Locks, Conn.